2013 IEEE/RSJ International Conference on
Intelligent Robots and Systems (IROS)
November 3-7, 2013. Tokyo, Japan

Evaluations on Contribution of Backdrivability and Force Measurement Performance on Force Sensitivity of Actuators*

Hiroshi Kaminaga[1], Kohei Odanaka[1], Yuta Ando[1], Satoshi Otsuki[1], and Yoshihiko Nakamura[1]

Abstract— **The importance of force measurement and backdrivability in realizing force sensitive actuator is widely acknowledged. There are studies on fidelity of torque sensors and backdrivability individually, but limited study are made on investigating effect of torque fidelity and backdrivability on force sensitivity of the actuation system. In this paper, we developed backdrivable electro-hydrostatic actuator equipped with torque sensor to analyze the effect of torque fidelity and backdrivability on force sensitive control system. We implemented friction compensation controller and evaluated force sensitivity of the actuator by residual friction torque after the friction compensation. Method using pressure sensor and torque sensor were compared. Effect of backdrivability was performed by comparing friction torque of Harmonic Drive joint and joint with developed actuator.**

I. Introduction

In early days of robotics, vast majority of the control objective was to follow the desired trajectory as precisely as possible. The joints were high-gain position controlled to follow given trajectory of either an end-effector or each joints. The term "robustness" was used for disturbance rejection capability of trajectory following. On the other hand, applications as prosthetic devices, which interact with human, have always considered the flexibility of the device as fundamental requirement of physical interaction. The importance of physical human robot interaction has increasing importance, not only in prosthetic devices, but also in service robots. Now, even the industrial robots are expected to work together with human operators.

The flexibility, mentioned above, implies force sensitivity since desired task cannot always be accomplished only being flexible; joint must generate adequate torque. For the robots to be force sensitive, robots must feel the applied force. Tactile sensing is the simplest way, but in general, total force acting on the robot is difficult to be measured only with tactile sensors. The most common method of force control is the use of 6-axis force sensor mounted on the wrist of the end-effector[1]. There are also works to install joint torque sensors as [2], [3], which enables the robot to make contact with environment at any link of the robot. This method has good property from the collocation point of view.

However, force (torque) sensor based force control, with few exceptions, rely on control to realize force sensitivity. Admittance control [4] is commonly used in force sensor based force control, but in practice it is known to have stability issue when the robot makes hard contact. Impedance control is known to be more stable, but it requires backdrivability of the actuator system. Backdrivability is the passive property of the actuator system that the output axis of the actuator can be driven passively with external force applied to output axis[5]. This property is not guaranteed in all actuator systems due to the friction in the system. Normal worm gears are known to be non-backdrivable [1]. Non-backdrivable actuators are also called to have "self locking" property, which is useful in some cases. In non-backdrivable actuators, force control must be done through position control, which limits the controllability. Hence for robots to be truly force sensitive, actuator must be backdrivable.

There are works on torque sensors as listed previously. There are works on backdrivability as well[6], [7], [5]. However, there were few research that investigate contribution of force measurement performance and backdrivability on system's force sensitivity.

Our aim of this paper is to investigate contribution and effect of torque sensing and backdrivability on force sensitive control systems. To accomplish the objective, we developed an backdrivable electro-hydrostatic actuator with a torque sensor we named "torque encoder"[8]. In this paper, we first explain the structure of the developed actuator. We then evaluated how the use of torque encoder affects the torque sensitivity by comparing performance of friction compensation on the developed actuator.

II. Electro-Hydrostatic Actuators (EHAs) and Force Sensitive Control on EHAs

Electro-Hydrostatic Actuators (EHAs) are displacement control type hydraulic systems that usually consist of a pair of a hydraulic pump and a hydraulic motor.(SeeFig. 1). Unlike resistance control type hydraulic systems with servo valves, EHAs require no valve to control supply energy to the hydraulic motors. Instead, EHAs adjust either displacement or rotation of the pump to control amount of energy being supplied to hydraulic motors. In general, EHAs have significant advantage on efficiency due to its control principle and equivalent serial resistance. In this work, we used an EHA with fixed displacement pump to further reduce the friction, size, and weight to be suitable as a robot actuator.

EHA reduces speed and gains torque with Pascal's principle and difference in moment arm. Pumps have small

*This work was supported by Grant-in-Aid for Young Scientists (B) (No. 23760219) of the Japan Society for the Promotion of Science.

[1]H. Kaminaga, K. Odanaka, Y. Ando, S. Otsuki, and Y. Nakamura are with Department of Mechano-Informatics, Graduate School of Information Science and Technology, The University of Tokyo, 7-3-1 Hongo, Bunkyo-Ku, Tokyo, 113-8656, Japan kaminaga@ynl.t.u-tokyo.ac.jp

[1]Worm gears also become backdrivable with appropriate design

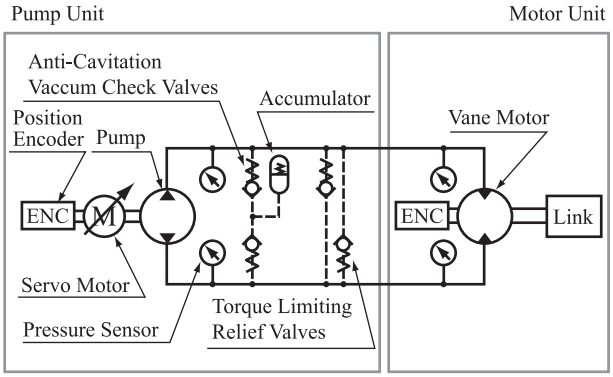

Fig. 1. Hydraulic Schematic of an Electro-Hydrostatic Actuator. Solid line shows main power transmission circuit and dashed line shows auxiliary circuit.

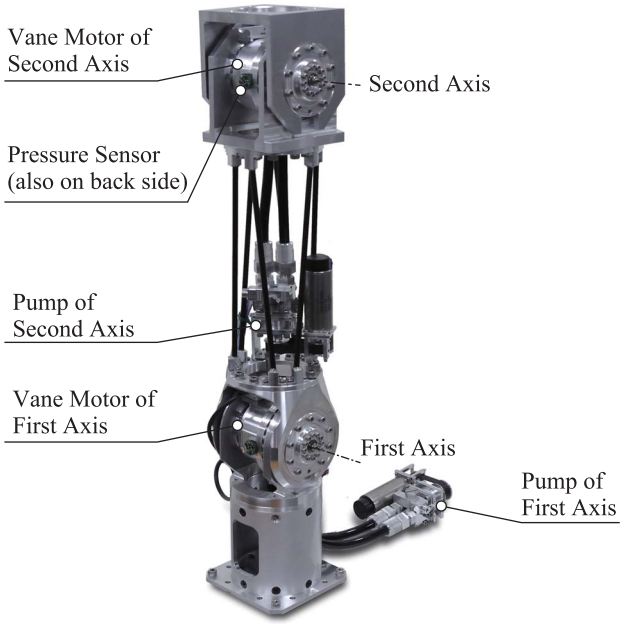

Fig. 2. Outlook of the EHA in 2-Link Configuration

surface area and small moment arm, where hydraulic motors typically have large surface area and large moment arm. Since there is no friction involved in the reduction process, transmission friction becomes small compared to gear drives, especially the reduction ratio is high. This low friction property enhances backdrivability of the actuation system. In our work, we intentionally allow very small amount of internal leakage in the hydraulic motor and in the pump. This internal leakage reduces friction and introduces underactuated degree of freedom that decouples pump side and hydraulic motor side dynamics. This decoupling enhances backdrivability[9].

In the developed actuator, we followed basic concept of our previous work [10] that combines trochoid type inner gear pump and double vane rotary hydraulic motor. Outlook of the actuator system in 2-link configuration is shown in Fig. 2.

Our fundamental objective is to develop backdrivable actuator. In general, contact seals are used in hydraulic pumps and motors to enhance volumetric efficiency. Since contact seals introduce large friction, we avoid the use of contact seals except for seal at pump input axis and hydraulic motor output axis. We want to have minimum clearance between rotating components to have minimum internal leakage, which degrades transmission efficiency. Large internal leakage is not necessary from backdrivability point of view. On the other hand, small clearance increases viscous frictional force from drag, which also degrades transmission efficiency. They are contradicting conditions. However, the internal leakage flow rate is proportional to cubic of the gap where the drag force in inverse proportional to the gap. Vane tips were carefully designed using this principle.

For the force sensitive controller, friction compensation based on disturbance observer[11], [12] was used. This method was first introduced by De Luca et al.[13] as fault detection in manipulator, which was then applied to friction compensation by Tien et al. [11]. We proposed the application of this method on EHA[12]. In [11], output torque was measured with a torque sensor. In an EHA, output torque can be estimated with pressure sensors, which are small and very rigid. However, the use of pressure sensor have disadvantage that it cannot observe nor compensate the friction at the output axis seal.

We estimate pump friction $\tau_{1\mathrm{f}}$ with (1), where $\hat{\tau}_{1\mathrm{f}}$ is the estimated value of the friction.

$$\tau_1 = J_1\ddot{\hat{\theta}}_1 + k_{13}p_1 + \hat{\tau}_{1\mathrm{f}} \quad (1)$$

$$\hat{\tau}_{1\mathrm{f}} = -LJ_1\left(\dot{\theta}_1 - \dot{\hat{\theta}}_1\right) \quad (2)$$

Here, L is the observer gain and k_{13} is the constant that converts pump discharge pressure p_1 to pump torque τ_1 in static state. $\hat{\theta}_1$ is the observer state. The estimate $\hat{\tau}_{1\mathrm{f}}$ converges to $\tau_{1\mathrm{f}}$ with time constant $1/L$ as stated in [13], [11].

As an implementation, (3) is used instead of (1) to compensate friction from hydraulic tubes.

$$\tau_1 = J_1\ddot{\hat{\theta}}_1 + k_{13}p_2 + \hat{\tau}_{1\mathrm{f}} \quad (3)$$

The estimated friction $\hat{\tau}_{1\mathrm{f}}$ is added to desired input torque in feed-forward manner to compensate the friction.

III. Structure of Torque Encoders

Output axis torque sensors can measure torque acting on output axis. The issues of using a torque sensor on a robot are size, weight, and elasticity. To have high sensitivity measurement, following combinations are possible: (a) low stiffness flexure and no filter (b) rigid flexure and low bandwidth filter. Method (a) increases the signal magnitude to enhance signal to noise (S/N) ratio. Method (b) suppresses noise to enhance S/N ratio. In either cases, delay is introduced in the control system that limits control bandwidth. As a result, dynamic performance is sacrificed. This trade-off is the innate property of the torque sensing and control.

The key to overcome this trade-off is to enhance sensing S/N ratio. The most commonly used sensing device in torque

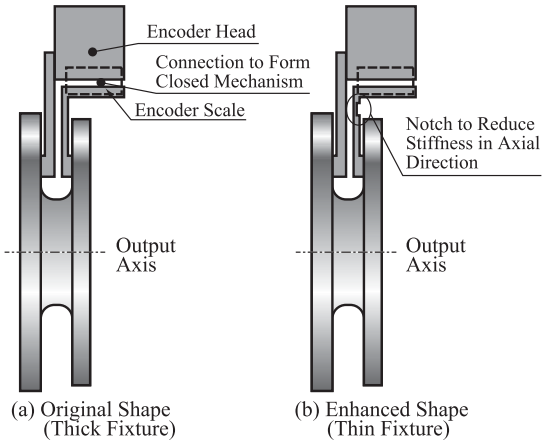

Fig. 3. Mechanical Structure of Fixtures to Realize Different Fixture Thickness

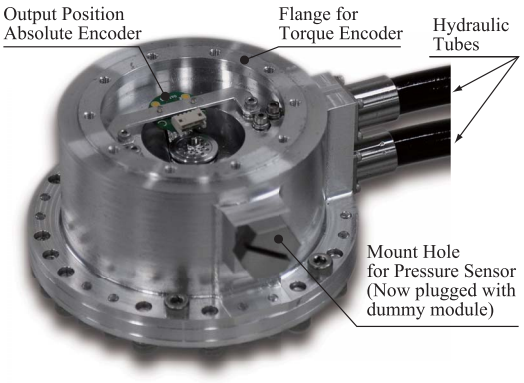

Fig. 4. Flange Side of Vane Motor

sensors are strain gauges [14] and optical detectors[15], [16]. However, these sensors require delicate analog signal processing, which is likely to have low noise immunity. Kawakami et al. [8] developed "*Torque Encoders*" that sense torque with high resolution linear encoder. Linear encoders are, from its principle, robust against noise contamination. We succeeded in realizing S/N ratio 7 times higher compared to that of strain gauge torque sensors. We have investigated in the mechanism to suppress crosstalk element of the torque measurement for torque encoders as in [17]. Measurement crosstalk is the measurement interference of non-measurement direction 5 axis forces.

To suppress crosstalk in torque encoder, relative stiffness between the encoder head and the scale must be high in all direction except for the measurement direction. Or in other word, stiffness between the encoder head or scale and the flexure must be low in these directions. In previous study [17], it was realized by using fixture with different thickness so that the stiffness between the encoder head and the flexure becomes high and the stiffness between the scale and the flexure becomes low. In this paper, we modified the encoder scale fixture to further decouple axial load acting between encoder head and scale. This is done by introducing a notch on a fixture holding the scale as shown in Fig. 3.

Friction compensation using torque encoder is similar to the friction compensation with pressure sensors as shown in (1) and (2). The difference is that instead of using $k_{13}p_2$ for output torque estimation, output torque can directly be measured with the torque encoder. Putting the measured output torque τ_1^*, the disturbance observer is given by (4) and (5).

$$\tau_1 = J_1\ddot{\hat{\theta}}_1 + \tau_1^* + \hat{\tau}_{1\mathrm{f}} \quad (4)$$

$$\hat{\tau}_{1\mathrm{f}} = -LJ_1\left(\dot{\theta}_1 - \dot{\hat{\theta}}_1\right) \quad (5)$$

IV. EHA WITH TORQUE ENCODER

Our objective of this paper is to investigate the contribution of backdrivability and torque measurement performance in force sensitivity of a robot actuator. In order to achieve this objective, we need to combine high sensitivity torque sensor with high backdrivability actuator. We developed backdrivable EHA with torque encoder.

With a torque encoder, we can measure output torque without the measurement error of output axis oil seal friction, which we cannot be eliminated with pressure sensors based output torque estimation. However, there are more advantages. EHA have high actuator system stiffness because there is no elastic element as harmonic drive flexspline. To maintain this stiffness, torque sensor also is required to have high stiffness. From this point of view, torque encoder is suitable torque sensing device for EHA.

We designed EHA for manipulator as shown in Fig. 2. Based on the design in [10], we scaled up the power capacity from 100W in [10] to 200W that is presented in this paper. There are some design variations from [10] to make the actuator suitable for manipulator purpose.

1) Opposite side to output axis was made to have flange surface to mount torque encoder
2) Tubes leading out from the vane motor is placed on cylinder surface to have space on both sides to be used for fixing the actuator to the links
3) Use double angular bearing support to realize high rigidity

Fig. 4 shows the outlook of the developed vane motor. The simplified joint structure is shown in Fig. 5. Fig. 6 shows developed torque encoder that fits to the EHA. One side of the torque encoder is designed to serve as bearing axis to minimize size and weight of the actuator. Table I shows specifications of the developed torque encoder. The pump looks almost identical to that of [10], just motor and pully being modified. Table II shows specification of the designed EHA.

V. EXPERIMENT

A. Crosstalk Evaluation

To measure the amount of crosstalk, external torque was applied in the direction perpendicular to the measurement direction. Applied external torque was measured with a force gauge. Ideally, output from torque encoder should show 0 regardless the external torque, but in reality, some amount of

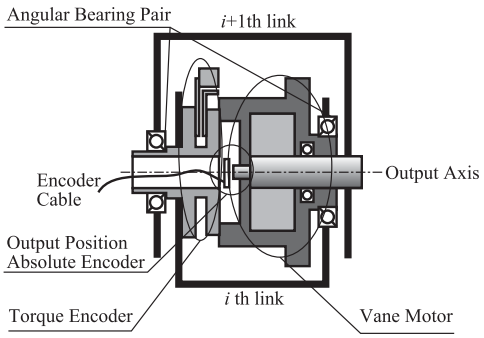

Fig. 5. Conceptual Cross Section of EHA Driven Joint Mechanism with Torque Encoder

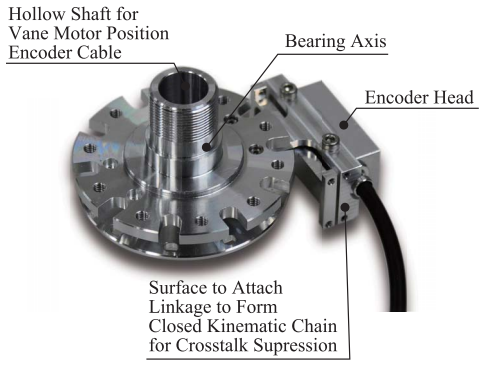

Fig. 6. Structure of Torque Encoder for EHA

the torque is observed as crosstalk. We used next equation as the evaluation value of crosstalk.

$$\hat{\tau}_{\mathrm{x}} = \max_{\tau_{\mathrm{i}}} |\tau_{\mathrm{x}}(\tau_{\mathrm{i}})| \tag{6}$$

Here, applied torque is τ_{i}, amount of measured torque is $\tau_{\mathrm{x}}(\tau_{\mathrm{i}})$, and $\hat{\tau}_{\mathrm{x}}$ is the evaluation value of the crosstalk.

The result of the evaluation is shown in Table III. In the table, "No Mechanism" means the case without crosstalk suppression mechanism. "Original Mechanism" means the case with the fixture in [17]. "Proposed Mechanism" is the result of proposed structure. From the result, use of proposed

TABLE I

SPECIFICATIONS OF TORQUE ENCODER FOR EHA

Description	Value	Units
Sensing Resolution	6×10^{-3}	Nm
Diameter	92×10^{-3}	m
Torsional Stiffness	5.0×10^{4}	Nm/rad
Safety Factor	8.3	
Material	7000 Series Aluminum Alloy	

TABLE II

SPECIFICATION OF DEVELOPED EHA

Description	Value	Units
Max. Output Torque	60	Nm
Max. Rotational Speed	6.9	rad/s
Range of Motion	120	deg

TABLE III

COMPARISON OF CROSSTALK FOR DIFFERENT FIXTURE THICKNESS

Method	Crosstalk (Nm)	Reduction (%)
No Mechanism	5.48	-
Original Mechanism[2]	2.67	58
Proposed Mechanism	1.88	66

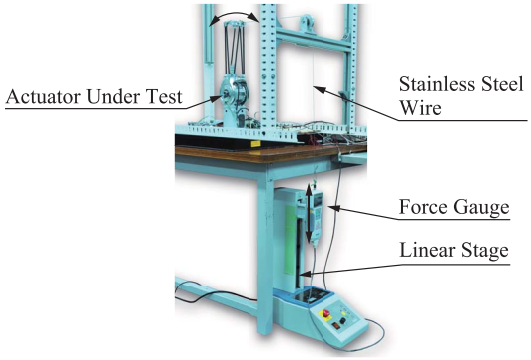

Fig. 7. Friction Torque Evaluation Test Apparatus

structure showed 8% less crosstalk compared to the original mechanism [2] .

B. Friction Compensation in Small Movements

To evaluate force sensitivity of actuators, we used residual friction torque after friction compensation as a measure. Active and passive property were examined to investigate effect of backdrivability and torque sensing performance. The evaluation was done with the test apparatus shown in Fig. 7. Displacement was applied to actuator with wire connected to the force gauge, which is mounted on a linear stage that moves with constant speed. Applied torque was calculated from the measured wire tension and joint angle.

First, behavior from stop to moving state was examined. Actuator was pulled with the speed of 2.19×10^{-3}rad/s. The result is shown in Fig. 8 and Table IV.

The test started from the wire being slack, resulting input torque being 0 in the beginning. The reason that the friction torque rise smoothly in Fig. 8 is slackness and elasticity of the wire. From the result, we can see that the pressure based friction compensation does not operate at this low speed. This is due to the lack of sensitivity of the pressure sensors that they could not detect the applied force; resultant pressure is proportional to applied velocity when there is internal leakage. On the other hand, when the torque encoder was used, direct output axis torque sensing was effective in detecting the external force. Residual friction torque was reduced to 1.2% of non-controlled case.

As the evaluation of backdrivability, we applied torque to non-controlled Harmonic Drive joint [8] in same way. The

[2]The reduction of the crosstalk was calculated against data for each mechanism since changing fixture involves disassembly, which would affect amount of the crosstalk. Amount of the crosstalk for no mechanism and original fixture were 6.4Nm.

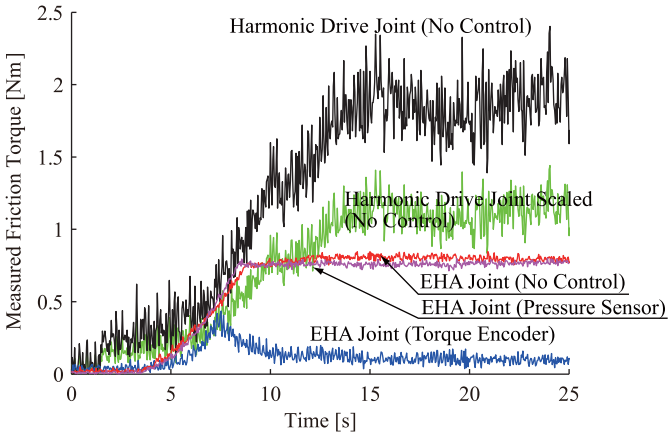

Fig. 8. Comparison of Friction Torque from Static State

TABLE IV
COMPARISON OF FRICTION TORQUE

Case		Friction Torque (Nm)	
Actuator	Control	Static	Coulomb
EHA	No Control	0.77	0.77
	Pressure Sensor Feedback	0.79	0.79
	Torque Encoder Feedback	0.43	0.093
Harmonic	No Control	2.0	2.0
	No Control (Scaled with Max. Torque)	1.2	1.2

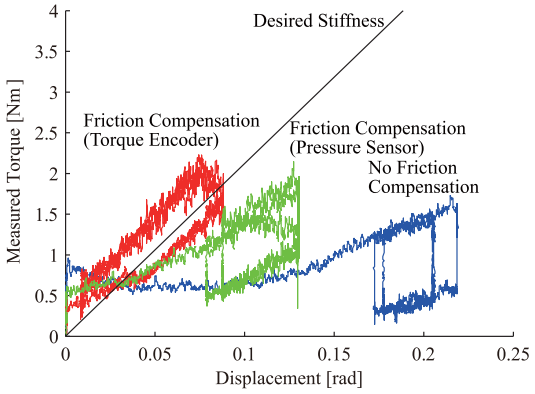

Fig. 9. Comparison of Compliance Control Behavior

TABLE V
COMPARISON OF REALIZED STIFFNESS

Case	Stiffness (Nm/rad)	Hysteresis (Nm)
Reference	21.2	
No Friction Compensation	7.34	0.915
Pressure Sensor Friction Compensation	8.00	0.827
Torque Encoder Friction Compensation	15.4	0.720

difference in S/N ratio comes from the difference in force gauge used. Harmonic drive joint required larger torque to backdrive that required the use of force gauge with different range. However, this was not fair comparison because the maximum output torque differs between the EHA and Harmonic Drive joint. To make the comparison fair, we scaled the result of Harmonic Drive joint with the maximum torque. This result is labeled "Harmonic Drive Joint Scaled." Still, from the result, passive friction torque was 36% lower than that of scaled data of Harmonic Drive joint. We also observed smoother friction torque from EHA. The fluctuation of the friction of Harmonic Drive is expected to come from the movement of the wave generator in Harmonic Drive.

C. Friction Compensation in Larger Movements

Next, we observed the difference in behavior of friction compensation methods for larger movements. To avoid the wires getting slack, we used compliance control to give pretension to the wire. This time, since the stroke of the linear stage was not sufficient, displacement were manually given.

Fig. 9 shows angle-torque relation of the result. Fig. 10 shows time series data of single forward-backward motion extracted from second hysteresis loop of Fig. 9. The displacement was given with same speed to previous test with small error, which is $2.19\times10^{-3}\mathrm{rad/s}$. This can be observed from bottom figure of Fig. 10. The amount of friction was estimated from the exerted torque τ_e and desired torque $\tau_\mathrm{d} = K\theta$, where K is the desired stiffness and θ being the angular displacement. Estimated friction torque is given with $\tau_\mathrm{f} = \tau_\mathrm{d} - \tau_\mathrm{e}$.

From Fig. 9 and Fig. 10, we can observe stable behavior of the friction compensation at larger movement. Friction torque of the case without friction compensation shows large friction torque from the friction in the pump, which is magnified by the reduction ratio in observation. In larger movement, pressure based friction compensation is active. The friction compensation reduces the pump friction, but still maximum friction torque of $2\mathrm{Nm}$ is observed. This comes from uncompensated friction of the pump and output axis oil seal. The positive correlation of friction toque and desired torque comes from uncompensated viscous friction in the pump. We can roughly see the difference in friction torque of pressure based control and torque encoder based control as the friction torque of output axis oil seal. Exerted torque in the beginning does not becomes 0 due to the static friction of previous movement.

From this evaluation, we can also observe accuracy of the force control. Result is shown in Table V. From the result, we can see the effect of friction compensation for both torque encoder and pressure sensor. We observe reduction in amount of hysteresis and and accuracy of realized stiffness. The difference between torque encoder and pressure sensor is in torque encoder, friction of output axis can be compensated where it is not possible with pressure sensors.

VI. CONCLUSIONS

The objective of this paper was to investigate contribution and effect of torque sensing and backdrivability in force

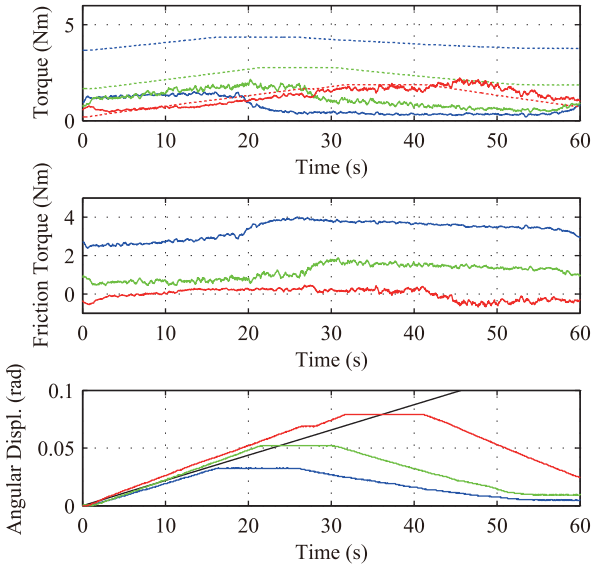

Fig. 10. Friction Torque Evaluation for Large Movement. Blue: No control, Green: Pressure Based, Red: Torque Encoder Based. Solid lines in top figure shows exerted torque. Dotted lines show desired torque from compliance control. Middle figure shows friction torque estimated from observed torque and desired torque. Bottom figure shows angular displacement from beginning of the movement. Black line in bottom figure shows 2.19×10^{-3} rad/s.

sensitive control systems by evaluating force control performance on one backdrivable actuator with multiple force sensors with different property. We developed an backdrivable electro-hydrostatic actuator with torque encoder and implemented friction compensation controller that use pressure sensors and torque encoder for comparison. Followings are the conclusions of this paper.

1) Developed EHA with suitable structure to be used in manipulator. Design of the EHA was performed with scalability.
2) Developed torque encoder to be used with EHA. Crosstalk suppression mechanism reduced crosstalk by 66%. The suppression performance enhanced by 8% compared to previous method.
3) Under low speed ($2.19\times10^{-3}\mathrm{rad/s}$) with 0 torque control, pressure sensor based friction compensation was not effective. This is due to the torque sensing property of pressure sensors that sensitivity is dependent on the velocity.
4) Torque encoder based friction compensation reduced residual friction by 98.8%.
5) Friction in passive backdriving in EHA was 64% of that of Harmonic Drive, which shows the high backdrivability of EHA.
6) At larger movement, both pressure sensor and torque encoder were effective. This is due to compliance control, which generated momentum at pump, which is necessary in disturbance observer being used. Accuracy and hysteresis were best with torque encoder. This is due to the fact that torque encoders can measure output axis oil seal friction that is possible with pressure sensors.
7) Output axis torque sensing is effective when the physical accuracy of the force control and accuracy in low speed is important. Pressure sensor is effective for application that is too small to use torque encoders. In all cases, high backdrivability actuator is desirable.

REFERENCES

[1] D. E. Whitney, "Resolved Motion Rate Control of Manipulators and Human Prostheses," *IEEE Trans. on Man-Machine Systems*, vol. 10, no. 2, pp. 47–53, 1969.

[2] R. Paul, "Modeling, Trajectory Calculation, and Servoing of a Computer Controlled Arm," Ph.D. dissertation, Computer Science Department, Stanford University, 1972.

[3] G. Hirzinger, N. Sporer, A. Albu-Schäffer, M. Hähnle, R. Krenn, A. Pascucci, and M. Schedl, "DLRfs torque-controlled light weight robot III - are we reaching the technological limits now?" in *Proc. of IEEE Int'l Conf. on Robotics and Automation*, 2002, pp. 1710–1716.

[4] N. Hogan, "Impedance Control: An Approach to Manipulation: Part I-III," *Trans. of ASME J. Dyn. Sys. Meas. Ctrl*, vol. 107, no. 1, pp. 1–23, 1985.

[5] H. Kaminaga, J. Ono, Y. Nakashima, and Y. Nakamura, "Development of Backdrivable Hydraulic Joint Mechanism for Knee Joint of Humanoid Robots," in *Proc. of IEEE Int'l Conf. on Robotics and Automations*, 2009, pp. 1577–1582.

[6] M. Zinn, O. Khatib, B. Roth, and J. K. Salisbury, "Playing It Safe," *IEEE Robotics and Automation Mag.*, vol. 11, no. 2, pp. 12–21, 2004.

[7] T. Ishida and A. Takanishi, "A robot actuator development with high backdrivability," in *Proc. of IEEE Conf. on Robotics Automation and Mechatronics*, 2006, pp. 1–6.

[8] T. Kawakami, K. Ayusawa, H. Kaminaga, and Y. Nakamura, "High-fidelity joint drive system by torque feedback control using high precision linear encoder," in *Proc. of IEEE Int'l Conf. on Robotics and Automation*, 2010, pp. 3904–3909.

[9] H. Kaminaga, T. Amari, Y. Katayama, J. Ono, Y. Shimoyama, and Y. Nakamura, "Backdrivability Analysis of Electro-Hydrostatic Actuator and Series Dissipative Actuation Model," in *Proc. of IEEE Int'l Conf. on Robotics and Automations*, 2010, pp. 4204–4211.

[10] H. Kaminaga, T. Amari, Y. Niwa, and Y. Nakamura, "Development of Knee Power Assist using Backdrivable Electro-Hydrostatic Actuator," in *Proc. of IEEE/RSJ Int'l Conf. on Intelligent Robots and Systems*, 2010, pp. 5517–5524.

[11] L. Tien, A. Albu-Schäffer, A. De Luca, and G. Hirzinger, "Friction Observer and Compensation for Control of Robots with Joint Torque Measurement," in *Proc. of IEEE/RSJ Int'l Conf. on Intelligent Robots and Systems*, 2008, pp. 3789–3795.

[12] H. Kaminaga, H. Tanaka, and Y. Nakamura, "Mechanism and Control of Knee Power Augmenting Device with Backdrivable Electro-Hydrostatic Actuator," in *Proc. of 13th World Congress in Mechanism and Machine Science*, no. A12_534, 2011, pp. 1–10.

[13] A. D. Luca and R. Mattone, "Actuator Failure Detection and Isolation Using Gneralized Momenta," in *Proc. of IEEE Int'l Conf. on Robotics and Automation*, 2003, pp. 634–639.

[14] I. Godler, M. Hashimoto, and M. Horiuchi, "Performace of gain-tuned harmonic drive torque sensor under load and speed conditons," *IEEE/ASME Trans. on Mechatronics*, vol. 6, no. 2, pp. 155–160, 2001.

[15] S. Hirose and K. Yoneda, "Development of Optical Six-Axial Force Sensor and its Signal Calibration Considering Nonlinear Interference," in *Proc. of IEEE Int'l Conf. on Robotics and Automation*, vol. 1, 1990, pp. 46–53.

[16] D. Tsetserukou, R. Tadakuma, H. Kajimoto, and S. Tachi, "Optical Torque Sensors for Local Impedance Control Realization of an Anthropomorphic Robot Arm," *Int'l J. of Robotics and Mechatronics*, vol. 18, no. 2, pp. 121–130, 2006.

[17] H. Kaminaga, K. Odanaka, T. Kawakami, and Y. Nakamura, "Measurement Crosstalk Elimination of Torque Encoder Using Selectively Compliant Suspension," in *Proc. of IEEE Int'l Conf. on Robotics and Automations*, 2011, pp. 4774–4779.